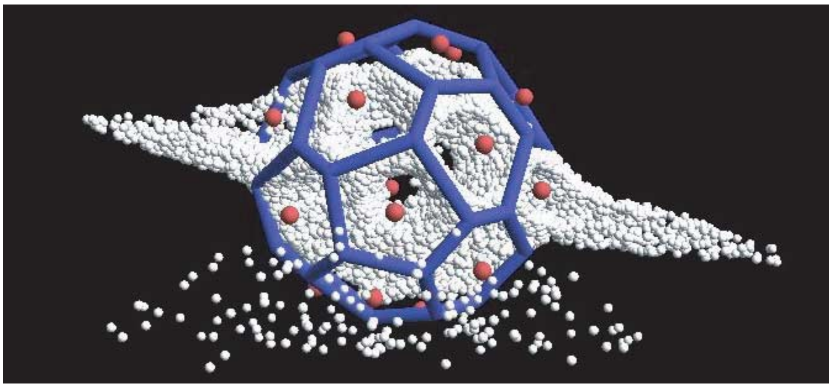

Fig. 8. Results of the procedure with the original 3D image of *Pantanellium* B. Red spheres indicate the centers of the pores.

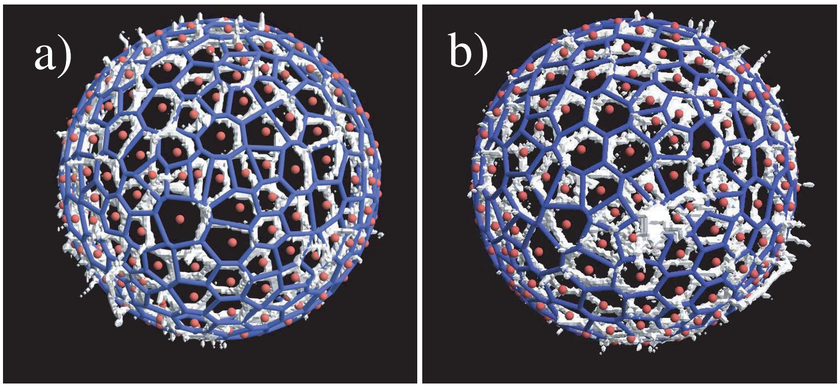

Fig. 9. Results of the procedure with the original 3D image of *Haliommilla*. Red spheres indicate the centers of the pores.

where n_i is the number of neighbors of the i-th grid point, and the summation is carried out for the neighbors of the i-th grid point. This transformation is applied simultaneously to all the grid points. In this study, we repeated the filter three times. After this procedure, we discretized the values x_i to 0 or 1, according to the appropriate threshold value.

3. Results

In order to validate our proposed method, as discussed in the previous section, we prepared three 3D data sets obtained from micro X-ray CT scans. These were obtained from two different specimens of *Pantanellium* and one specimen of modern radiolaria *Haliommilla*. All of the specimens were about 10^{-4} m in length. The first was the STL data set of *Pantanellium*, shown in Fig. 1, and the results for this are shown in Fig. 5. We will refer this as *Pantanellium* A. The second was the TIFF data of another *Pantanellium*, shown in Fig. 6. The skeleton-forming points are represented by small spheres. This data set has noise due to the micro X-ray CT scanning process. Although some of this noise can be removed by converting from TIFF to STL, it cannot be removed completely, so we used this data to examine the robustness of our procedure. We refer to this data set as *Pantanellium* B. The third data were the STL data of *Haliommilla*, shown in Fig. 7. The images in Fig. 7 were also obtained from same STL data, but the viewpoint is different. In Fig. 7b, the back of the hemisphere was omitted for clarity. This specimen had many pores and a thin frame, compared with those of the two *Pantanellium* specimens, and it was impossible to count the pores by visual inspection. Furthermore, as shown in Fig. 7b, these data contained some errors around the center of the image. Without the use of the smoothing filter, neither of the last two data sets produced correct results. We use the word "correct" to describe the inherent properties of the specimen.

Figure 8 shows the results of applying the method to the original 3D image of *Pantanellium* B. We used a geodesic grid with $N = 16$ (2,562 grid points). We applied the smoothing filter because these data contain some noise. The red spheres indicate the centers of the pores, and the blue frame shows the result of the Voronoi tessellation of the centers of the pores. As shown in Fig. 8, the approximated polyhedron agreed with the original data. The estimated number of pores was 24. This value was also consistent with the one obtained by visual inspection.

For *Haliommilla* (Fig. 9), we did not obtain the correct number of pores because the one-to-one correspondence between pores and generators was broken in some regions, as shown in Fig. 9b. The images in Fig. 9 were taken using same viewpoint as those in Fig. 7. We used a geodesic grid with $N = 128$ (163,842 grid points) and applied the smoothing filter. The estimated number of pores was 262. As shown in Fig. 9a, determination of the pores was apparently successful in most regions. There was, however, a questionable region near the center of the image, as shown in Fig. 9b. Therefore, we conclude that, in this case, our procedure was insufficient for estimating the appropriate structure.